ACS APPLIED MATERIALS & INTERFACES
Research Article
www.acsami.org

Graphene Oxide Film as Solid Lubricant

Hongyu Liang,[†,‡] Yongfeng Bu,[†] Junyan Zhang,[*,†] Zhongyue Cao,[†,‡] and Aimin Liang[†]

[†]State Key Laboratory of Solid Lubrication, Lanzhou Institute of Chemical Physics, Chinese Academy of Sciences, Lanzhou 730000, China

[‡]University of Chinese Academy of Sciences, Beijing 100049, China

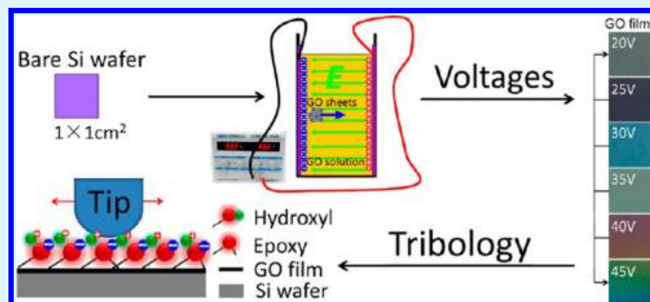

ABSTRACT: As a layered material, graphene oxide (GO) film is a good candidate for improving friction and antiwear performance of silicon-based MEMS devices. Via a green electrophoretic deposition (EPD) approach, GO films with tunable thickness in nanoscale are fabricated onto silicon wafer in a water solution. The morphology, microstructure, and mechanical properties as well as the friction coefficient and wear resistance of the films were investigated. The results indicated that the friction coefficient of silicon wafer was reduced to 1/6 its value, and the wear volume was reduced to 1/24 when using GO film as solid lubricant. These distinguished tribology performances suggest that GO films are expected to be good solid lubricants for silicon-based MEMS/NEMS devices.

KEYWORDS: *graphene oxide film, electrophoretic deposition, adhesion, friction, wear, solid lubricant*

1. INTRODUCTION

Micro/nanoelectromechanical systems (MEMS/NEMS) are considered to be useful in many areas such as microsensors, microactuators, microrobots, and micro power systems;[1] however, the severe wear is becoming the biggest challenge for the moving parts in MEMS/NEMS,[2,3] since the current fabrication approaches for MEMS/NEMS devices mainly depend on the existing semiconductor manufacturing techniques that use silicon materials as raw materials, which are well-known to be worn easily.[2,4] Therefore, good lubrication has become a crucial issue for exerting the MEMS/NEMS performance reliablely. In consideration of the small dimensions of the MEMS/NEMS devices, lubricating the moving parts inside the devices is much more difficult than any parts of traditional mechanical systems. Apparently, liquid lubricants are incompatible with MEMS/NEMS because of the precision requirements of devices, and a solid lubricant on the surface of moving parts is coming up as a choice.[5,6]

As solid lubricant to MEMS/NEMS, good thermal stability, low friction coefficient, high wear resistance, and controllable thickness are required. In view of a solution-based manufacturing process, organic self-assembled monolayers (SAMs) such as hydrocarbon and fluorocarbon SAMs films have been paid much attention as lubricants for MEMS/NEMS to reduce the adhesion and friction in the last decades.[7,8] However, the SAMs suffer from many vital shortages, such as poor wear resistance, poor preparation reliability, and poor thickness modulation, indicating that SAMs are not suitable to be surface lubricants in practice for MEMS/NEMS. With intrinsic mechanical strength and lower shear force similar to graphite, graphene may be a good solid lubricant because of its layer structural features.[9−11] Recently, it was reported that the chemical vapor deposition (CVD) grown graphene film could be considered as the thinnest solid lubricant.[11] However, CVD-grown graphene films need high growth temperature and metal substrates such as Cu and Ni foils, simultaneously, this technique faces the problem of the film transferring to silicon based MEMS/NEMS parts.[12,13] As a solution-based process, electrophoretic deposition (EPD) has been applied successfully for the deposition of graphene film with the help of Mg^{2+} as charger to render graphene sheets positively charged.[14,15] However, additive magnesium salts may break the stability of the electrolyte, and even weaken the tribological performance of the film. With layer structure and some similar properties to graphene and graphite, graphene oxide (GO) film may be a good solid lubricant to MEMS/NEMS. Furthermore, without any charged additives, graphene oxide sheets can form a stable water based colloidal solution as a result of the negative charges repulsion of oxygen-containing groups on the GO sheets.[16] Therefore, highly pure GO film (without containing metal ions) could be obtained via electrophoretic deposition because the negatively charged GO sheets always move to the anode, in contrast, metal ions (even present) migrate toward the cathode under an electric field. Moreover, the deposition area and thickness of GO films could be adjusted according to the needs, including the area of fine structures of MEMS/NEMS parts which are difficult to infiltrate using traditional coating methods.

Herein, we have prepared GO film on silicon substrate via EPD, the reusults indicated that the GO films exhibited good mechanical and tribological properties, such as high hardness,

Received: April 23, 2013
Accepted: June 6, 2013
Published: June 20, 2013

© 2013 American Chemical Society

Scheme 1. Schematic of Electrophoretic Deposition for Preparation of GO Film on Silicon Substrate

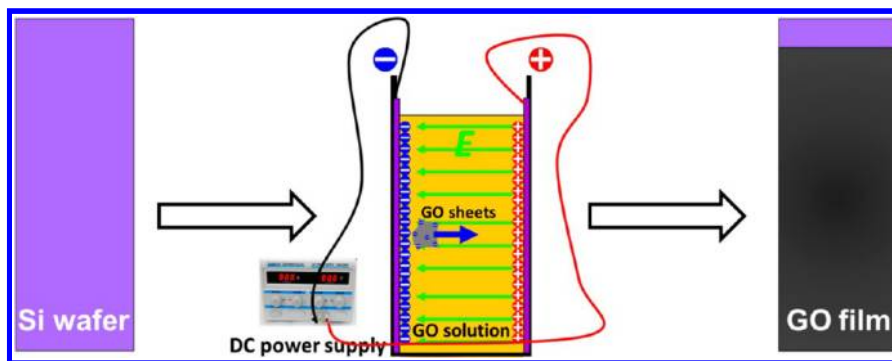

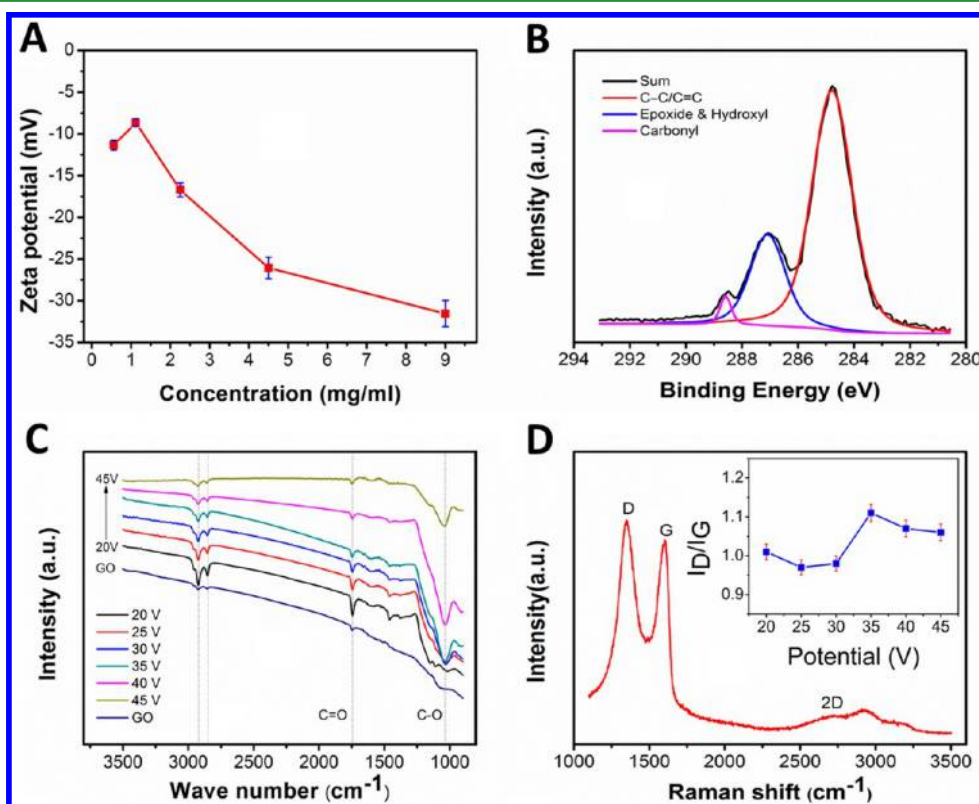

Figure 1. (A) Zeta potential of GO colloidal solutions of various concentrations. (B) XPS spectrum of C1s for GO sheets. (C) Reflection IR spectra of GO raw material and films deposited on silicon substrates at different voltages (20−45 V). (D) Typical Raman spectra of the GO film deposited 35 V. Inset shows the relative ratios of I_D/I_G of the GO films deposited at various voltages (20−45 V).

high recovery, lower friction coefficient, and good wear resistance. With GO film as solid lubricant, the friction of the silicon wafer was reduced to 1/6 its value, and the wear was reduced to 1/24. It demonstrated that the GO films could reduce the friction and wear of silicon significantly.

2. EXPERIMENTAL SECTION

2.1. Materials. Graphene oxide was synthesized from nature graphite (320 mesh) purchased from Sigma (USA). N-type polished single-crystal silicon (100) wafers with resistivity of 0.01were purchased from MCL Electronic Materials, Ltd. Ultrapure water (>18 MΩ cm^{-1}) used throughout the experiment was purified using a Milli-Q system from Millipore Co.

2.2. Preparation of GO Films. GO used in this study was prepared by Hummers method.[17,18] After that, the GO powder was dispersed into ultrapure water with the aid of sonication, to generate a uniform and stable GO colloid solution. Prior to deposition, silicon wafers were cleaned in a piranha solution (a mixture of 98% H_2SO_4 and 30% H_2O_2 with the ratio of 7:3 (v/v)), subsequently washed with ultrapure water several times and blown dry with N_2. A simple electrophoretic deposition system was used to prepare GO films, it was showed in Scheme 1. Two symmetric silicon wafers were employed as work electrodes that immersed into a beaker containing 4.56 mg/mL GO colloid aqueous solution, with a constant distance of 5 mm. The cell was then connected to a DC power supplying with various voltages of 20, 25, 30, 35, 40, and 45 V for an hour, and the corresponding films were denoted as GOF20, GOF25, GOF30, GOF35, GOF40, and GOF45, respectively. All of the experiments were carried out at room temperature (22 °C).

2.3. Characterization. The values of zeta potential of GO colloid solutions were measured by Laser dynamic scattering tester (Nano ZS 3600, Malvern, England). After deposition, the topographies of GO films were observed by microscope (Olympus, Japan) and scanning electron microscopy (FE-SEM, JSM-6701F, JEOL, Japan). The thickness measurements were performed with a L116-E ellipsometer (Gaertner, America), which is equipped with a He−Ne laser (632.8 nm) set at an incident angle of 50°. A real refractive index of 1.25 is set

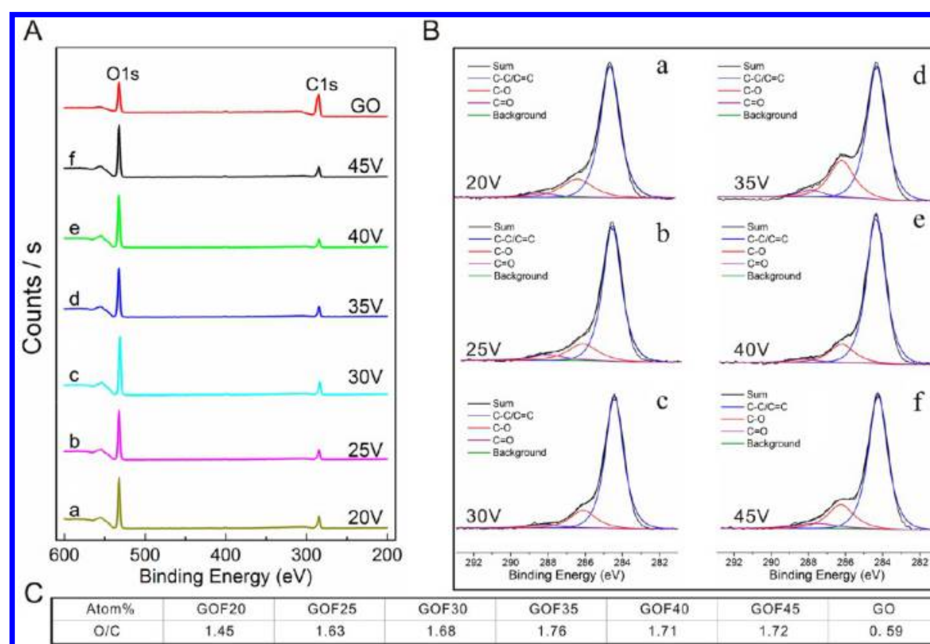

Atom%	GOF20	GOF25	GOF30	GOF35	GOF40	GOF45	GO
O/C	1.45	1.63	1.68	1.76	1.71	1.72	0. 59

Figure 2. XPS spectra of (A) survey and (B) C1s for GO films deposited under different voltages (20−45 V), and (C) table with respect to the ratio of oxygen atoms to carbon atoms in the GO films.

for the silica layer. In addition, transmission electron microscopy (TEM, JEM-1200EX, JEOL, Japan), Raman spectroscopy (JY-HR800, the excitation wavelength at 532 nm), Nexus 870 FTIR spectrometer (Nicolet), and X-ray photoelectron spectroscopy (XPS, ESCALAB 250Xi, Thermon Scientific) were applied to reveal the structure and component of the deposited films. To obtain the adhesion of the film to the silicon wafer, the friction−load curve was recorded on a multifunctional material surface performance tester (MFT-4000). The loading force corresponding to the mutation site of friction was considered to be the adhesion. The mechanical properties of the films were measured by a nanoindenter (TI-950, Hysitron, USA) equipped with a Berkowich diamond tip which is a three-sided pyramid with tip angle of 142.3°. The indentation depth was set below 10% of the film thickness in order to minimize the substrate influence on the film mechanical property. Five repeated indentations were made for each sample and the hardness and Young's modulus were calculated from the loading−unloading curves. The elastic recovery was calculated from the formula $R = (d_{max}-d_{res})/d_{max}$, where d_{max} and d_{res} are the maximum and minimum displacements during loading and unloading, respectively. The stiction was measured by AFM (AIST-NT,Smart-SPM, USA) with a tip parameters as follows: the force constant was 0.1, slope was 1.5 and the applied force was 1.33 nN. All experiments were carried out at room temperature (22 °C).

2.4. Tribological Study of the GO Films. Tribological tests were performed on a reciprocating ball-on-plate tester (MFT-R4000) at room temperature in ambient air. Commercially available steel balls (φ = 3 mm, mean roughness = 0.02 μm) were used as the stationary upper counterparts, whereas the lower tested samples were mounted onto the flat base and driven to slide reciprocally at a distance of 2.5 mm. The normal load for all tests were 400 mN, and the reciprocating frequencies were all 5 Hz. The friction coefficient versus time curves were recorded automatically and the friction coefficient for each sample was determined by the average of continuously examining data. The wear tracks were examined by a surface three-dimensional profiler (ADE, USA). All tests were performed at least three times to ensure the repeatability of the deposited films.

3. RESULTS AND DISCUSSION

3.1. Preparation and Characterization of GO Films. GO aqueous solution is an inherent negatively charged colloidal solution due to the presence of residual polar oxygen-containing groups on the GO sheets. Figure 1A shows the zeta potential of GO colloidal solution in different concentrations that the values of zeta potential are all negative (from −8 to −32 mV) and decrease with increasing concentration, which confirms that GO sheets scattered in water are charged with negative charges due to the oxygen-containing groups on the GO sheets. These oxygen-containing groups were identified by XPS (Figure 1B) that C−O (hydroxyl and epoxy groups, ∼287.1 eV) and C═O (carbonyl group, ∼288.6 eV)[19] are the main oxygen-containing groups.[20] That is, we can directly take advantage of these inherently negative charges on GO sheets and make them move to the oppositely charged electrode to fabricate GO films in a water solution under an electric field. To further investigate the chemical structure of these films, we employed reflection IR spectra and Raman spectrum. The IR peaks located at ∼1744 and ∼1037 cm^{-1} are ascribed to the C═O and C−O stretching vibrations (Figure 1C), respectively. In comparison with GO sheets (blue curve), IR spectra illustrate that various voltages have little discernible effect on the chemical constitutions of GO sheets except on the C−O peak intensity. Simultaneously, this point is also confirmed by Raman spectrum. In the Raman spectrum of the GO film (Figure 1D), two prominent peaks at ∼1348 (D mode) and∼1603 cm^{-1}(G mode) were observed, and the intensity ratio of I_D/I_G varied with applied voltages and reached to the highest value at 35 V (inset in Figure 1D). The increase of I_D/I_G is generally the reflection of disorder increase in the GO sheets,[21] which could be attributed to strong oxidation of the positive pole under high working voltages. To investigate the effect of applied deposition voltages on chemical changes in the GO films, we conducted the XPS spectra of survey and C1s for the as-prepared GO films deposited at different voltages and displayed in panels A and B in Figure 2. It shows that C−O (hydroxyl and epoxy groups, ∼287.1 eV) and carbonyl carbon C═O (∼288.6 eV) are the main components except the carbon skeletons C−C or C═C (∼284.8 eV), which are agreed with the GO sheets composition. The O/C ratios were obtained from the corresponding peak areas in the XPS (Figure

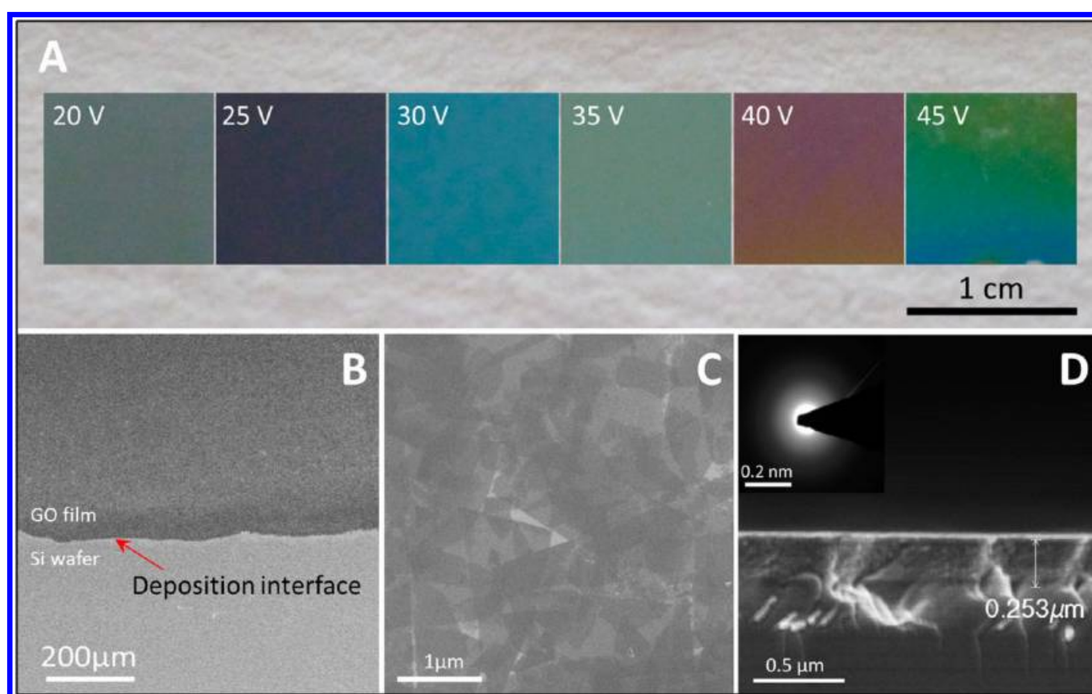

Figure 3. (A) Optical images of GO films deposited on silicon wafers for 1 h at different voltages (20−45 V) by electrophoresis in GO colloidal solution. (B) Low-magnification SEM image of the GO film (35 V) with a clear deposition interface. (C) High-magnification SEM image of the GOF 20 film. (D) Cross-sectional SEM image and SAED pattern (inset) of the GOF35 film.

2A). It was found that the O/C ratios ranging from 1.63 to 1.76 for GO films (Figure 2C) were all greater than the raw materials of the GO sheets (O/C = 0.59). On the whole, the changes of GOF35, GOF40 and GOF45 were higher than the low voltages samples such as GOF20, GOF25 and GOF30. Among them, GOF35 (35 V) had the biggest change that may be attributed to the strong oxidation ability of the positive pole during electrophoresis. What is important is that the O/C changing trend was consistent with that of Raman I_D/I_G ratios, which further demonstrated the existence of strong oxidation occurred on the GO films. So from this point of view, lower voltages may be favorable to maintain the original quality of GO films.

As shown in Figure 3A, the colors of as-prepared GO films vary with the applied voltages. This phenomenon could be attributed to the variation of the film thickness. The films thicknesses measured by ellipsometer were 50, 99, 171, 259, 296, and 402 nm corresponding to the samples of GOF20, GOF25, GOF30, GOF35, GOF40, and GOF45, respectively. With increasing thickness, longer wavelengths of light are absorbed and the films' color changed from gray (GOF20) to bluish (GOF25) and eventually fuchsia (GOF40). Figure 3B shows a homogeneous film (the upper part of the SEM image) with clear deposition boundary (the sample immersing line in solution) on the bare Si wafer, which means that GO film could be deposited easily on the surface uniformly. Furthermore, without any charged additives in the solution, the deposition process with only water as medium is a green and environment friendly fabrication approach. Figure 3C shows a typical SEM image of the GO film (GOF20) composed of the overlapping GO sheets, demonstrating that the GO film is layered three-dimensional stack of GO sheets instead of the mixture of erect and flat sheets, which results in a lower RMS roughness (0.59 nm). However, the GO sheets tend to corrugation or wrinkle, which led the RMS roughness up to 2.61 nm (Table 1) when

Table 1. Roughness, Stress, and Stiction of the GO films Deposited at Different Voltages

sample	roughness (nm)	stress (GPa)	stiction[a] (nN)
GOF20	0.59	4.66	59.68
GOF25	1.38	2.04	40.71
GOF30	1.43	1.59	1.08
GOF35	1.65	−0.20	1.17
GOF40	2.61	−0.25	1.09
GOF45	2.75	−0.32	0.82

[a]Stiction (adhesion) was measured by AFM using a probe to contact the GO film surface.

the voltage reached to 40 V. Figure 3D shows a typical cross-section view of the GO film in which the film is very dense without evident defects and the thickness is about 253 nm, well agreeing with 259 nm measured by ellipsometer. The diffraction pattern of GOF35 in inset of Figure 3D shows the typical character of GO sheets.[22] The poor-defined diffraction rings in selected area electron diffraction (SAED) pattern illustrate that the crystalline state of the GO film is amorphous, unlike graphene or graphite with well-defined diffraction spots in SAED. It confirms that there are defects in the GO films unambiguously. Figure 4A shows the load−displacement curves of the GO films from the nanoindentation measurements, the hardness and Young's modulus of the GO films both increase with the increase of applied working voltage (Figure 4B), which is probably due to the fact that the deposition speed of the GO sheets is faster at higher working voltage and the higher impact makes the GO film more dense with higher hardness and higher Young's modulus. However, the film surface is becoming rougher at higher working voltage, as shown in Table 1. GOF35 possesses the hardness of 5 GPa and elastic recovery of 74.8%, whereas GOF40 and GOF45 have relatively higher hardnesses but a little bit lower elastic recoveries. Compared with silicon

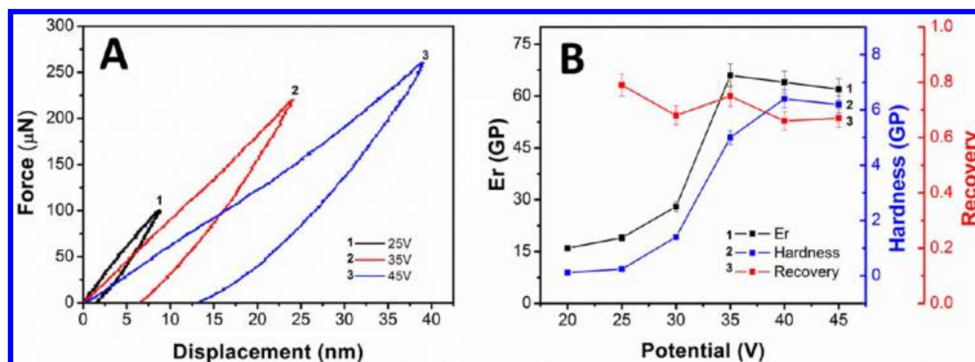

Figure 4. (A) Three typical nanoindentation force−displacement curves for GO films depositedon at 25, 35, and 45 V. (B) Hardnesses, elastic moduluses, and elastic recoveries of the GO films versus various voltages (20−45 V), respectively.

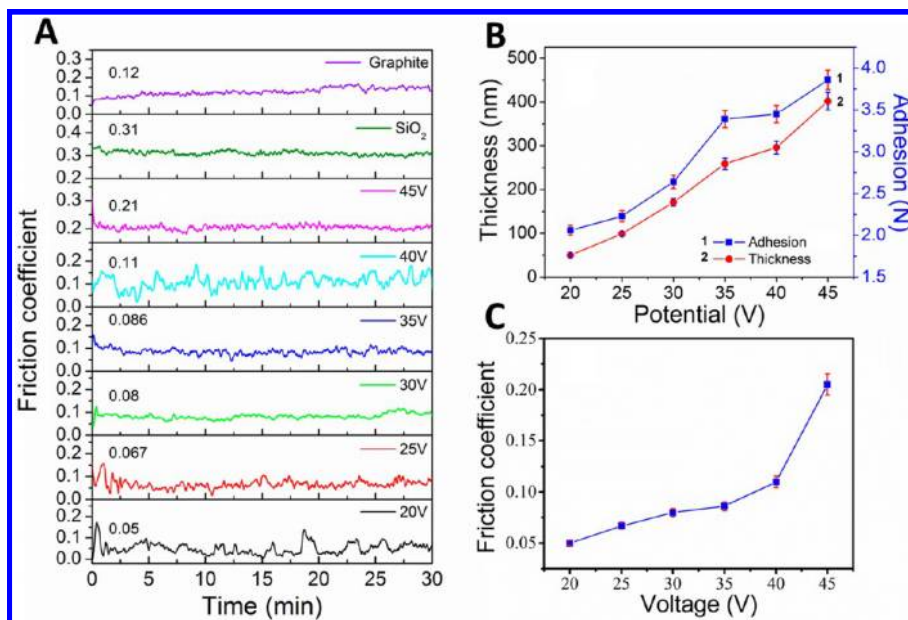

Figure 5. (A) Variations in friction coefficient with time (friction conditions: load = 400mN, frequency = 5 Hz, distance = 2.5 mm, time = 30 min) for graphite flake, bare silicon wafer and GO films deposited at different voltages (20−45 V). (B) Thicknesses and adhesion to silicon substrate and (C) friction coefficients of the GO films as a function of voltages, respectively.

wafer with the hardness of about 12 GPa, the GO films are soft films with several GPa hardness.

3.2. Friction and Wear Behaviors of the GO Films. As mentioned above that GO films may serve as solid lubricants for MEMS/NEMS, and the fact that the GO films are soft compared with silicon wafer implies that the GO films would not bring harsh wear to silicon during friction process.[23] The tribological properties of the GO films were investigated by ball-on-disk test. Figure 5A shows the friction curves of the samples in which the GO films demonstrated lower friction coefficients compared with silicon wafer, 0.05, 0.067, 0.080, 0.086, 0.11, and 0.21, corresponding to GOF20, GOF25, GOF30, GOF35, GOF40, and GOF45, respectively. The friction coefficient of the GO film increases with the increase in surface roughness, whereas the surface roughness increases with the increase of applied voltage (Table 1). That means the friction coefficient of the GO film could be controlled or adjusted to some extent by applied voltage. The friction coefficient of GOF20 is only one-sixth that of the silicon wafer that means the GO film could significantly reduce the friction of Si and could be considered as potential solid lubricant for MEMS/NEMS. To compare friction behavior, we investigated a graphitic flake under the same conditions (Figure 5A). The result indicated that the friction coefficient of the graphite flake was about 0.12, which is close to that of GO40, and 1.4 times and 2.4 times higher than that of GOF35 and GOF20, respectively. However, the wear volume of graphitic flake (3.19×10^{-12} m^3) is much higher than that of the GO films (3.38×10^{-14} m^3 for GOF35). This further supports that the GO films could serve as solid lubricant to Si based MEMS/NEMS devices. Additionally, there is a linear relationship between the film thickness and the applied voltage that the higher voltage the thicker the film is (Figure 5B). The adhesion of the GO films to Si substrates has the same tread with the film thickness that the adhesion increases from about 2.1 to 3.8 N with the increase of the film thickness (Figure 5B), probably caused by stronger impact effect at higher working voltage. Considering the low lateral shearing force of MEMS parts, this level adhesion is able to meet the requirement for the solid lubricant of MEMS.[24] The stiction (adhesion) of the GO film can be measured by AFM using a probe to contact the film surface. The related results were listed in Table 1. It displays that the variation of surface stiction is inversely proportional with roughness under the same applied force. The decreased

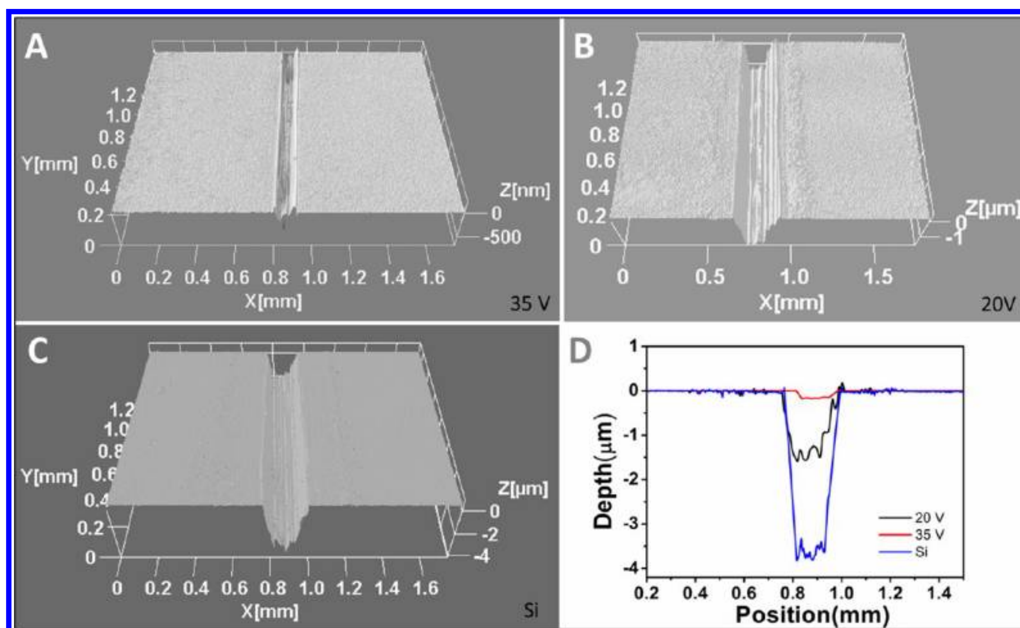

Figure 6. 3D images of the wear tracks of GO films deposited at 35 V (A) and 20 V (B), and a bare silicon wafer (C), and corresponding surface profiles (D), respectively. Friction test conditions were as follows: load = 400 mN, frequency = 5 Hz, distance = 2.5 mm, and time = 30 min.

adhesive force of GO film surface is due to the reduced real area of contact. For instance, GOF20 with a minimum roughness (0.59) results in a maximum stiction (59.68 nN). On the whole, it is clear that the stiction force is very high at lower applied voltage while the stiction force is very low at higher applied voltage, 1.08, 1.17, 1.09, and 0.82 nN for GOF30, GOF35, GOF40, GOF45, respectively. Such low stiction forces at higher applied voltages are favorable to the smooth motion of MEMS/NEMS devices.

For a solid lubricant, the wear-resistance ability is also crucial to their practice application in MEMS/NEMS devices since the severe wear would damage the MEMS parts leading to the failure of the system.[25] Figure 6 shows 3D profiles of the wear tracks of silicon wafer, GOF20 and GOF35 films, respectively, which reveal that the bare silicon wafer is badly worn and the wear track is up to 3.5 μm in depth (Figure 6C). However, the wear tracks for GOF20 and GOF35 are much shallower, 1.5 and 0.12 μm in depth, respectively (Figures 6A, B). According to the thickness of GOF20, 50 nm measured by ellipsometer, it can be concluded that the GOF20 had been worn out completely, whereas the GOF35 is still there. Additionally, the internal stress test results showed that the internal stress of the GO films reached to close to zero at higher applied voltages, about 0.2 GPa for GOF35 (Table1), and the highest stress (4.66 GPa) of GOF20 may be the reason to the poor wear resistance, since the higher stress may induce the breaking and peeling off of the GO film during the friction process. However, GOF35, with the wear depth of 120 nm (within its thickness of 259 nm), exhibited good wear resistance that may result from the lowest stress of 0.2 GPa.[26] This also demonstrates that EPD technique is a green and robust approach for preparing films used in silicon-based MEMS/NEMS devices.

The wear volume of silicon wafer was 8.32×10^{-13} m^3, whereas the wear volume of GOF35 was 3.38×10^{-14} m^3, 1/24 of that of silicon, and much lower than that of graphite flake (3.19×10^{-12} m^3), which means that the GO film could prolong the wear life of silicon significantly. For GOF40 and GOF45, though with low wear volumes, they have high surface roughness and higher friction coefficients which make them unsuitable for the smooth moving of the fine parts of MEMS/NEMS devices.[27] Combing with the friction and wear behaviors, it is clearly that the GO film fabricated at 35 V exhibited good performance both in friction and wear resistance, and hence, GO films fabricated via EPD have potential to be good candidates as solid lubricants in MEMS/NEMS devices.

4. CONCLUSIONS

In summary, pure GO film, fabricated directly on silicon substrates via green and environment friendly EPD technique without any charged additives (only water as medium), could be served as a common MEMS parts solid lubrication material. The thickness of the GO film could be controlled by adjusting the working voltage. The higher working voltage led to harder and rougher films, and the adhesion of the film to silicon substrate was also enhanced by higher working voltage. The friction coefficient of the film seems to be correlated to the roughness of the film that the rougher film generates higher friction coefficient, whereas the wear resistance of the GO film is improved by higher working deposition voltage probably deriving from more dense film produced at higher voltage. In a word, the GO film fabricated via EPD could reduce the friction and prolong the wear life of silicon significantly. GO film is a good candidate with potential to be solid lubricant for MEMS/NEMS devices.

■ AUTHOR INFORMATION

Corresponding Author

*E-mail: zhangjunyan@licp.cas.cn. Tel./fax: +86 9314968295.

Notes

The authors declare no competing financial interest.

■ ACKNOWLEDGMENTS

This work was supported by Key Basic Research Project of China (973 Program, 2013CB632300), National Natural Science Foundation of China (51275508, 51205383).

REFERENCES

(1) Bishop, D.; Pardo, F.; Bolle, C.; Giles, R.; Aksyuk, V. *J. Low Temp. Phys.* **2012**, *169*, 386−399.
(2) Ku, I.; Reddyhoff, T.; Holmes, A.; Spikes, H. *Wear* **2011**, *271*, 1050−1058.
(3) Subhash, G.; Corwin, A. D.; de Boer, M. P. *Tribol. Lett.* **2011**, *41*, 177−189.
(4) Shen, S.; Meng, Y. *Tribol. Lett.* **2012**, *47*, 273−284.
(5) Gellman, A. J. *Tribol. Lett.* **2004**, *17*, 455−461.
(6) Donnet, C.; Erdemir, A. *Tribol. Lett.* **2004**, *17*, 389−397.
(7) Mikulski, P. T.; Van Workum, K.; Chateaueuf, G. M.; Gao, G.; Schall, J. D.; Harrison, J. A. *Tribol. Lett.* **2011**, *42*, 37−49.
(8) Lewis, J. B.; Vilt, S. G.; Rivera, J. L.; Jennings, G. K.; McCabe, C. *Langmuir* **2012**, *28*, 14218−14226.
(9) Thomas, P.; Delbé, K.; Himmel, D.; Mansot, J. L.; Cadoré, F.; Guérin, K.; Dubois, M.; Delabarre, C.; Hamwi, A. *J. Phys. Chem. Solids* **2006**, *67*, 1095−1099.
(10) Filleter, T.; McChesney, J. L.; Bostwick, A.; Rotenberg, E.; Emtsev, K.; Seyller, T.; Horn, K.; Bennewitz, R. *Phys. Rev. Lett.* **2009**, *102*, 86102−86106.
(11) Kim, K. S.; Lee, H. J.; Lee, C.; Lee, S. K.; Jang, H.; Ahn, J. H.; Kim, J. H.; Lee, H. J. *ACS Nano* **2011**, *5*, 5107−5114.
(12) Chandross, M.; Lorenz, C. D.; Grest, G. S.; Stevens, M. J.; Webb, E. B., III. *JOM* **2005**, *57*, 55−61.
(13) Song, H.-J.; Li, N. *Appl. Phys. A: Mater. Sci. Process.* **2011**, *105*, 827−832.
(14) Gao, B.; Yue, G. Z.; Qiu, Q.; Cheng, Y.; Shimoda, H.; Fleming, L.; Zhou, O. *Adv. Mater.* **2001**, *13*, 1770−1773.
(15) Wu, Z.-S.; Pei, S.; Ren, W.; Tang, D.; Gao, L.; Liu, B.; Li, F.; Liu, C.; Cheng, H.-M. *Adv. Mater.* **2009**, *21*, 1756−1760.
(16) Li, D.; Muller, M. B.; Gilje, S.; Kaner, R. B.; Wallace, G. G. *Nat. Nanotechnol.* **2008**, *3*, 101−105.
(17) Hummers, W. S.; Offeman, R. E. *J. Am. Chem. Soc.* **1958**, *80*, 1339−1339.
(18) Nair, R.; Wu, H.; Jayaram, P.; Grigorieva, I.; Geim, A. *Science* **2012**, *335*, 442−444.
(19) Becerril, H. A.; Mao, J.; Liu, Z.; Stoltenberg, R. M.; Bao, Z.; Chen, Y. *ACS Nano* **2008**, *2*, 463−470.
(20) Su, C.-Y.; Xu, Y.; Zhang, W.; Zhao, J.; Tang, X.; Tsai, C.-H.; Li, L.-J. *Chem. Mater.* **2009**, *21*, 5674−5680.
(21) Paredes, J. I.; Villar-Rodil, S.; Solis-Fernandez, P.; Martinez-Alonso, A.; Tascon, J. M. *Langmuir* **2009**, *25*, 5957−5968.
(22) Stankovich, S.; Dikin, D. A.; Compton, O. C.; Dommett, G. H.; Ruoff, R. S.; Nguyen, S. T. *Chem. Mater.* **2010**, *22*, 4153−4157.
(23) Kim, K. S.; Zhao, Y.; Jang, H.; Lee, S. Y.; Kim, J. M.; Kim, K. S.; Ahn, J.-H.; Kim, P.; Choi, J.-Y.; Hong, B. H. *Nature* **2009**, *457*, 706−710.
(24) Laboriante, I.; Suwandi, A.; Carraro, C.; Maboudian, R. *Sens. Actuators, A* **2013**, *193*, 238−245.
(25) Luo, D.; Fridrici, V.; Kapsa, P. *Wear* **2010**, *268*, 816−827.
(26) Hogmark, S.; Jacobson, S.; Larsson, M. *Wear* **2000**, *246*, 20−33.
(27) Singh, R.; Satyanarayana, N.; Kustandi, T.; Sinha, S. *J. Phys. D: Appl. Phys.* **2011**, *44*, 015301.